JACS
JOURNAL OF THE AMERICAN CHEMICAL SOCIETY
Communication
pubs.acs.org/JACS

Remarkable Performance of Ir_1/FeO_x Single-Atom Catalyst in Water Gas Shift Reaction

Jian Lin,[†] Aiqin Wang,[†] Botao Qiao,[†] Xiaoyan Liu,[†] Xiaofeng Yang,[†] Xiaodong Wang,[†] Jinxia Liang,[‡] Jun Li,[‡] Jingyue Liu,*[,†,§] and Tao Zhang*[,†]

[†]State Key Laboratory of Catalysis, Dalian Institute of Chemical Physics, Chinese Academy of Sciences, Dalian 116023, China
[‡]Department of Chemistry, Tsinghua University, Beijing 100084, China
[§]Department of Physics, Arizona State University, Tempe, Arizona 85287, United States

Supporting Information

ABSTRACT: High specific activity and cost effectiveness of single-atom catalysts hold practical value for water gas shift (WGS) reaction toward hydrogen energy. We reported the preparation and characterization of Ir single atoms supported on FeO_x (Ir_1/FeO_x) catalysts, the activity of which is 1 order of magnitude higher than its cluster or nanoparticle counterparts and is even higher than those of the most active Au- or Pt-based catalysts. Extensive studies reveal that the single atoms accounted for ~70% of the total activity of catalysts containing single atoms, subnano clusters, and nanoparticles, thus serving as the most important active sites. The Ir single atoms seem to greatly enhance the reducibility of the FeO_x support and generation of oxygen vacancies, leading to the excellent performance of the Ir_1/FeO_x single-atom catalyst. The results have broad implications on designing supported metal catalysts with better performance and lower cost.

Water gas shift (WGS, $CO + H_2O \rightarrow CO_2 + H_2$) is an important reaction to produce hydrogen for chemical processing and to remove CO contamination in feed streams for ammonia synthesis and fuel cells.[1] Although Cu-based catalysts have been used commercially, they are sensitive to air and condensed water during frequent shutdown−restart operation cycles for a fuel processing device. Au- or Pt-group metal catalysts with reducible oxide support are promising new generation of WGS catalysts for their high activity at relatively low temperatures and good stability.[2] However, the high cost of noble metals has limited their industrial applications. On the other hand, the utilization efficiency of noble metals in conventional supported catalysts is far less than satisfactory. For example, only 50% of metal atoms are used for catalysis when the metal is dispersed as 2 nm fine particles.[3] Even more cumbersome is the case of WGS reaction, where Au or Pt metal particles seem to be merely spectators, while atomically dispersed Au or Pt cations are the active sites.[4] The atomically dispersed metal species usually account for <~10 wt % in conventional supported catalysts,[5] with most of the expensive metal wasted. Therefore, a better solution of significantly reducing the use of precious metal is to prepare supported single-atom catalysts (SAC).[6]

In SAC, the surface free energy of the highly dispersed metal species maximizes comparing with those of nanoparticles and subnanometer clusters. The single atoms can be stabilized by anchoring on the surface of oxide support in a form of metal−O−support bonding (e.g., Au−O−Ce,[5a] Pt−O−Al,[7a,b] Pd−O−Al,[7c] Pt−O−Na,[7d] Ag−O−Mn,[7e] etc.) or on another metal surface in the form of alloying (e.g., Au atoms on the top sites of Pd clusters).[8] Recently, we reported a practical Pt_1/FeO_x SAC that exhibited 2−3 times higher activity than its cluster counterpart and excellent stability in both CO oxidation and preferential oxidation of CO in H_2 atmosphere (PROX).[9] The structure defects and the hydroxyl groups derived from poorly crystallized and large-surface area FeO_x support seem to play a key role in stabilizing the Pt single atoms. The Pt−O−Fe bonding leads to positively charged, high-valent Pt atoms on the FeO_x surface.

In the present work, we use an improved method to prepare an Ir_1/FeO_x SAC with an Ir loading of merely 0.01 wt %. Supported Ir catalysts were found to exhibit excellent performances in reactions, such as CO oxidation, hydrogenation, and dehydrogenation,[10] however, they rarely showed high activity in WGS reactions when comparing with Au or Pt catalysts.[1] Herein, we find that this Ir_1/FeO_x SAC exhibits exceptionally high activity for WGS reaction despite extremely low loading of Ir; the reaction rate reaches as high as 43.4 $mol_{co}\ g_{Ir}^{-1}\ h^{-1}$ at 300 °C, which is 1 order of magnitude higher than its cluster and nanoparticle counterparts. The Ir_1/FeO_x catalyst thus represents one of the most active catalysts reported so far for WGS, and its activity is even superior to Au- and Pt-based catalysts. More importantly, through extensive analysis of higher loading catalysts containing single atoms, subnanometer clusters, and nanoparticles, we find that the single atoms dominate the total activity and serve as the key active sites for WGS reaction.

We prepared a series of Ir/FeO_x catalysts with different Ir loadings via a coprecipitation method as reported previously.[9] A different precipitation temperature (80 °C) was used to guarantee that all of the H_2IrCl_6 in the solution was precipitated and loaded onto the FeO_x support. The resulting SAC with Ir loading of 0.01 wt % is denoted as Ir_1/FeO_x while the other samples as Ir/FeO_x-*n*, where *n* represents the Ir loading. After

Received: August 19, 2013
Published: October 3, 2013

dx.doi.org/10.1021/ja408574m | J. Am. Chem. Soc. 2013, 135, 15314−15317

recovery, the precipitate was dried at 80 °C overnight and reduced in 10% H_2/He at 300 °C for 0.5 h before further characterization and activity test. The Ir loadings and the specific surface areas of the catalysts are listed in Table S1.

To obtain the size distributions of small Ir clusters, we used sub-Å resolution, aberration-corrected STEM (AC-STEM) to visually observe the dispersion and configuration of a series of Ir/FeO_x catalysts. Figure 1 shows representative HAADF-STEM images of four samples; more images are presented in Figures S1, S2. The Ir single atoms can be clearly identified (labeled with white circles) together with FeO_x particles with sizes of 10−20 nm for Ir_1/FeO_x. It also reveals that the individual Ir atoms occupy exactly the positions of the Fe atoms. Careful examination of different areas with different image magnifications shows exclusively Ir single atoms on FeO_x support (Figure S1). The success in fabricating Ir_1/FeO_x SAC may lie in the extremely low loading of Ir, significantly reducing the probability of short- and long-rang Ir−Ir interactions (the density of Ir atoms is estimated to be only 0.001 atoms nm^{-2}). In contrast, for the Ir/FeO_x-0.22 catalyst, the single atoms (white circles) coexist with clusters <1 nm (red circles for <0.5 nm and red squares for 0.5−1 nm). Statistical analysis of many images show the distribution of these Ir species based on observation frequency: 60% single atoms, 33% clusters of <0.5 nm, and 7% clusters of 0.5−1.0 nm. When the Ir loading was further increased to 0.32 wt %, the observation frequency in the range of 0.5−1.0 nm increased slightly while that of <0.5 nm decreased, but no aggregation to sizes >1 nm occurred. In contrast, the Ir/FeO_x-2.40 catalyst contains not only single atoms (27%) and clusters (35% for <0.5 nm clusters and 34% for 0.5−1.0 nm clusters) but also particles larger than 1 nm (4%). Although all these Ir/FeO_x samples were pretreated with 10% H_2/He at 300 °C which is 100 °C higher than that for Pt/FeO_x reported previously, there is no Ir cluster with sizes >2 nm, implying a critical diameter of ∼1 nm for highly dispersed Ir metal.[11]

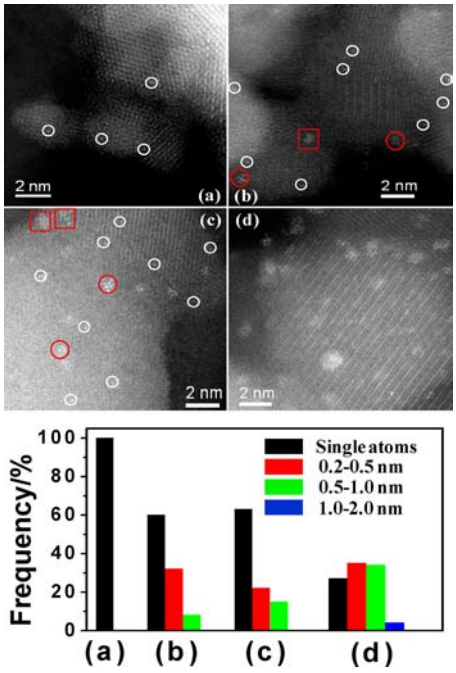

Figure 1. HAADF-STEM images and the frequencies of the observed size scope of Ir/FeO_x with the Ir loadings from 0.01 to 2.40 wt % (a) Ir_1/FeO_x; (b) Ir/FeO_x-0.22; (c) Ir/FeO_x-0.32; (d) Ir/FeO_x-2.40. The size distributions were obtained by analyzing 200−300 Ir species from high-magnification HAADF images (2 nm bar).

Consistent with the HAADF-STEM image analyses, XRD patterns of Ir/FeO_x samples (Figure S3) do not show any Ir-containing crystal phases. Correspondingly, one can observe typical Fe_3O_4 XRD patterns in all the Ir/FeO_x samples. Thus, the highly dispersed Ir, either as single atoms or clusters, was anchored onto Fe_3O_4 crystallites. The Ir/FeO_x samples were also characterized with X-ray absorption technique. Unfortunately, the Ir_1/FeO_x SAC did not show any signal due to its extremely low loading of Ir. Nevertheless, by analyzing the high-loading samples with X-ray absorption near-edge structure (XANES), we can clearly observe the trend that the Ir species become more positively charged with decreasing Ir loading (Figure S4). By extrapolating to the Ir_1/FeO_x, we concluded that the Ir single atoms were positively charged, in agreement with the result on Pt single atoms we reported earlier.[9]

The series of Ir/FeO_x samples were investigated for WGS at 300 °C, with a feed gas composition of 2% CO + 10% H_2O + He and a gas hourly space velocity of 18 000 mL g_{Cat}^{-1} h^{-1}. As shown in Figure 2a, the CO conversion is only 4% over the FeO_x support. However, after loading of Ir, even with an extremely low amount, the activity is increased significantly. The steady-state CO conversions arrived at 16%, 41%, 65%, and 93% over Ir_1/FeO_x, Ir/FeO_x-0.22, Ir/FeO_x-0.32, and Ir/FeO_x-2.40, respectively. It is noted that after excluding the contribution of the support, the CO conversion on the Ir/FeO_x-0.22 is only 3-fold higher than that on the Ir_1/FeO_x SAC, although the difference in Ir loading is 20-fold. This result indicates that in these reactions SAC is much more active than its cluster counterpart. To make a more realistic comparison, the specific reaction rates and turnover frequencies (TOFs) are measured in the kinetic region (by keeping CO conversion

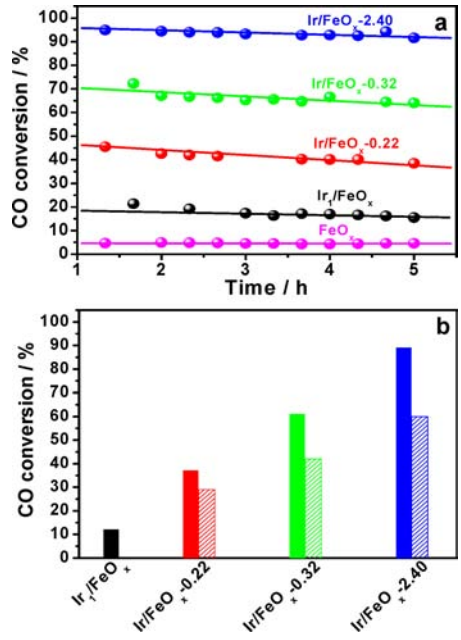

Figure 2. (a) CO conversions at 300 °C on the Ir/FeO_x catalysts with different Ir loadings, all samples were submitted to 300 °C reduction. (b) Differences between the experimental CO conversions at the steady state (solid column) and the estimated ones based on the contribution of Ir single atom sites (stripe column).

dx.doi.org/10.1021/ja408574m | J. Am. Chem. Soc. 2013, 135, 15314−15317

Table 1. Specific Rates and TOFs of Ir/FeO_x Catalysts Compared with the Reported Ir-, Pt-, and Au-Based Catalysts for WGS

catalyst	metal loading (wt%)	temperature (°C)	specific rate[a] (mol_{co} g_{NM}^{-1} h^{-1})	TOF (s^{-1})	E_a (kJ mol^{-1})	note
Ir_1/FeO_x	0.01	300	43.4	2.31[b]	50	this work
Ir/FeO_x	0.22	300	5.8	0.89[b]	53	this work
Ir/FeO_x	0.32	300	5.7	0.84[b]	54	this work
Ir/FeO_x	2.40	300	2.3	0.81[b]	52	this work
Pt_1/FeO_x	0.01	300	41.6	2.25[b]	-	this work
Ir/Al_2O_3	2.0	300	0.06	0.0032[c]	77	ref 12
Ir/TiO_2	5.0	350	0.12	0.029[c]	45	ref 12
Ir−Re(1:10)/TiO_2	1.0	200	0.08[d]	–	40	ref 13
Pt/MoC	3.9	240	20.4	1.42[e]	53	ref 14
Pt−Na/TiO_2	1	300	21.1	3.82[f]	80	ref 15
Au/CeO_x	0.28	300	11.9	0.65[g]	48	ref 4

[a]Reaction rates for all catalysts were collected at atmospheric pressure. [b]The Ir or Pt single atoms were completely dispersed on FeO_x for SAC, while for the loadings higher than 0.22 wt %, the Ir dispersions were determined by CO adsorption microcalorimetry and assumed that the stoichiometric ratio of adsorbed CO/Ir was 1. [c]Feed composition: 8% CO, 16% H_2O, bal. Ar. [d]Feed composition: 10% CO, 10% H_2O, bal. Ar. [e]Feed composition: 11% CO, 21% H_2O, 43% H_2, 6% CO_2, 19% N_2. [f]Feed composition: 2.83% CO, 5.66% H_2O, 37.74% H_2, bal. He; the Pt dispersion was determined by CO chemisorption, which was only 30%. [g]Feed composition: 11% CO, 7% CO_2, 26% H_2, 26% H_2O, bal. He. The Au/CeO_x was prepared by deposition precipitation, after that, the surface metallic Au was leached by NaCN solution, and the remaining ionic Au atoms were considered as complete dispersion on CeO_x support.

below 15%), and the results are summarized in Table 1. Surprisingly, the specific reaction rate of the Ir_1/FeO_x catalyst shows a remarkably high number of 43.4 mol_{co} g_{Ir}^{-1} h^{-1} at 300 °C, corresponding to a TOF of 2.31 s^{-1}. Such a high activity is almost 1 order of magnitude higher than its cluster counterparts. In comparison with other Ir catalysts reported in literature, such as Ir/Al_2O_3,[12] Ir/TiO_2,[12] or Ir−Re/TiO_2,[13] our Ir_1/FeO_x catalyst is 2−3 orders of magnitude more active. Even with the most active Pt or Au catalysts,[4,14,15] the Ir_1/FeO_x SAC has a comparable or even higher activity. To further demonstrate the superior performance of SAC, we prepared Pt_1/FeO_x SAC with Pt loading of 0.01 wt % and tested its activity for WGS reaction. As shown in Table 1 and Figure S5, the Pt_1/FeO_x SAC is also very active for the WGS reaction although its TOF is slightly smaller than that of the Ir_1/FeO_x SAC.

The Ir/FeO_x catalysts with higher loadings of Ir consist of not only clusters and particles but also single atoms. To clarify whether the single atoms therein dominate the total activity of the high-loading catalysts, we evaluated the contributions of single atoms to the WGS reaction based on the weight percentage of single atoms (calculation details in SI). The resulting percentages of single atoms in the Ir/FeO_x-0.22, Ir/FeO_x-0.32, and Ir/FeO_x-2.40 catalysts are 0.024, 0.035, 0.05, respectively. According to the steady CO conversion on the Ir_1/FeO_x SAC (0.01 wt % Ir loading), the CO conversions provided by each Ir single atom can be calculated. Then, the CO conversions afforded by the single atoms in the Ir/FeO_x-0.22, Ir/FeO_x-0.32, and Ir/FeO_x-2.40 catalysts could be obtained, yielding theoretically 29%, 42% and 60%, respectively. In comparison with the experimental values shown in Figure 2a (the activity contributed by support was excluded), one can clearly see that the Ir single atoms in these catalysts contribute around 70% to the total CO conversion (Figure 2b). Obviously, the Ir single atoms in the high-loading catalysts dominate their total activities. This result has provided strong evidence that the Ir single atoms are the most important active sites herein.

The kinetic tests further confirm the dominant role of single atom sites. As shown in Figure S6 and Table 1, the activation energies for the four samples are almost the same, 50−54 kJ mol^{-1}, which is significantly lower than that for bare FeO_x support (83 kJ mol^{-1}). The fact that the four catalysts contain different types of Ir entities but possess the same activation energy strongly suggests that the four catalysts have the same or similar type of active sites, in this case, the Ir single atoms.

The long-term stability, in particular at elevated temperatures, is crucial for the industrial application of SAC. Figure S7 shows the stability of the Ir_1/FeO_x SAC for WGS at 300 °C. The CO conversions remain constant (~30%) over 20 h run despite its slight decrease at the initial stage. The used catalyst was again checked by AC-STEM, and the result shows that it consists primarily of uniform Ir single atoms (Figure S8). Evidently, the Ir_1/FeO_x SAC is stable under typical WGS reaction conditions.

For the WGS reaction catalyzed by reducible oxide supported noble metals, it is generally accepted that CO adsorbs on noble metals while H_2O dissociates on oxygen vacancies of the reducible oxides.[16] Since the dissociation of H_2O molecules is a high-barrier step,[17] more oxygen vacancies will be favorable to this key step and then to the whole reaction rate of WGS.[18] The degree of generating oxygen vacancies can be evaluated from H_2 TPR. As shown in Figure S9, the presence of Ir single atoms leads to a significant lowering of the reduction temperature of the FeO_x support, from 315 °C on bare FeO_x to 270 °C on Ir_1/FeO_x catalyst. Moreover, we calculated the amount of H_2 consumed for FeO_x reduction as well as for IrO_2 and found that the ratio of the former to the latter arrived at the highest value for the Ir_1/FeO_x sample (Table S2). In comparison with its cluster counterparts, e.g., the Ir/FeO_x-2.40, this value was enhanced by 10-fold. These results strongly suggest that the Ir single atoms promote greatly the reduction of FeO_x, resulting in the generation of large amount of oxygen vacancies, which act as the sites for H_2O dissociation to produce H_2 and reactive oxygen species.

To understand this point, we conducted a TPSR experiment by exposing the samples with CO + H_2O at 300 °C. As shown in Figure S10, a low amount of CO_2 and H_2 was produced after exposing bare FeO_x support to the mixture of CO + H_2O. In contrast, a significant amount of CO_2 and H_2 was produced in the case of Ir_1/FeO_x catalyst, indicating that this SAC is highly active for WGS. Moreover, it was found that the production of H_2 always occurred before the production of CO_2, which

strongly suggested that H_2O was first activated on the FeO_x to produce H_2 and the reactive oxygen species, which subsequently reacted with CO adsorbed on Ir single atoms to produce CO_2. The abundance of oxygen vacancies in the reduced FeO_x support, which is greatly assisted by the presence of Ir single atoms, is likely responsible for the high activity for H_2O dissociation. Obviously, there is synergy between Ir single atoms and FeO_x. Herein, we would like to emphasize that the reducibility of the FeO_x support plays an important role in both stabilizing the Ir single atoms and contributing to the exceptionally high activity of Ir single atoms.

In summary, we have successfully fabricated Ir_1/FeO_x SAC with an exceptionally high activity for WGS, almost 1 order of magnitude higher than its cluster or nanoparticle counterparts. Such a performance is comparable with or even higher than the most active Au- or Pt-based catalysts. Through detailed analysis of higher loading Ir/FeO_x catalysts containing single atoms, subnanometer clusters, and nanoparticles, we have found that the single atoms contribute ~70% to the total activity. Thus, for the WGS reaction regardless of the loading amount, the single Ir atoms are the most important active sites in all the Ir/FeO_x catalysts that we prepared. These results have important implications for developing practical WGS catalysts, especially supported Ir catalysts. Further theoretical work on the fundamental catalytic mechanisms of Ir single atoms in WGS reaction is ongoing.

■ ASSOCIATED CONTENT

Supporting Information

Experimental section, catalyst preparation, water gas shift tests, AC-HAADF-STEM, ICP, BET, XRD, XANES, H_2 TPR, adsorption microcalorimetry, TPSR. This material is available free of charge via the Internet at http://pubs.acs.org.

■ AUTHOR INFORMATION

Corresponding Authors

jingyue.Liu@asu.edu
taozhang@dicp.ac.cn

Notes

The authors declare no competing financial interest.

■ ACKNOWLEDGMENTS

This work was supported by National Nature Science Foundation of China (21076211, 21203181, 21373206), the Hundred Talents Program of Dalian Institute of Chemical Physics and NKBRSF (2011CB932400). J.L. acknowledges the start-up fund of the College of Liberal Arts and Sciences of Arizona State University. The use of facilities in the John M. Cowley Center for High Resolution Electron Microscopy at Arizona State University and the beam line 14W at Shanghai Synchrotron Radiation Facility for EXAFS and XANES experiments are gratefully acknowledged.

■ REFERENCES

(1) Ratnasamy, C.; Wagner, J. *Catal. Rev.: Sci. Eng.* **2009**, *51*, 325.

(2) (a) Sakurai, H.; Ueda, A.; Kobayashi, T.; Haruta, M. *Chem. Commun.* **1997**, 271. (b) Hilaire, S.; Wang, X.; Luo, T.; Gorte, R.; Wagner, J. *Appl. Catal., A* **2001**, *215*, 271. (c) Tibiletti, D.; Meunier, F.; Goguet, A.; Reid, D.; Burch, R.; Boaro, M.; Vicario, M.; Trovarelli, A. *J. Catal.* **2006**, *244*, 183.

(3) (a) Bond, G. *Surf. Sci.* **1985**, *156*, 966. (b) Strizhak, P. *Theor. Exp. Chem.* **2013**, *49*, 2.

(4) Fu, Q.; Saltsburg, H.; Flytzani-Stephanopoulos, M. *Science* **2003**, *301*, 935.

(5) (a) Pierre, D.; Deng, W.; Flytzani-Stephanopoulos, M. *Top. Catal.* **2007**, *46*, 363. (b) Zhang, X.; Shi, H.; Xu, B. *Angew. Chem., Int. Ed.* **2005**, *44*, 7132. (c) Herzing, A.; Kiely, C.; Carley, A.; Landon, P.; Hutchings, G. *Science* **2008**, *321*, 1331.

(6) (a) Thomas, J.; Saghi, Z.; Gai, P. *Top. Catal.* **2011**, *54*, 588. (b) Flytzani-Stephanopoulos, M.; Gates, B. *Annu. Rev. Chem. Biomol. Eng.* **2012**, *3*, 545. (c) Yang, X.; Wang, A.; Qiao, B.; Li, J.; Liu, J.; Zhang, T. *Acc. Chem. Res.* **2013**, *46*, 1740.

(7) (a) Kwak, J.; Hu, J.; Mei, D.; Yi, C.; Kim, H.; Peden, C.; Allard, L.; Szanyi, J. *Science* **2009**, *325*, 1670. (b) Moses-DeBusk, M.; Yoon, M.; Allard, L.; Mullins, D.; Wu., Z.; Yang, X.; Veith, G.; Stocks, G.; Narula, C. *J. Am. Chem. Soc.* **2013**, *135*, 12634. (c) Hackett, S.; Brydson, R.; Gass, M.; Harvey, I.; Newman, A.; Wilson, K.; Lee, A. *Angew. Chem., Int. Ed.* **2007**, *46*, 8593. (d) Zhang, C.; Liu, F.; Zhai, Y.; Ariga, H.; Yi, N.; Liu, Y.; Asakura, K.; Flytzani-Stephanopoulos, M.; He, H. *Angew. Chem., Int. Ed.* **2012**, *51*, 9628. (e) Huang, Z.; Gu, X.; Cao, Q.; Hu, P.; Hao, J.; Li, J.; Tang, X. *Angew. Chem., Int. Ed.* **2012**, *51*, 4198.

(8) Zhang, H.; Watanabe, T.; Okumura, M.; Haruta, M.; Toshima, N. *Nat. Mater.* **2012**, *11*, 49.

(9) Qiao, B.; Wang, A.; Yang, X.; Allard, L.; Jiang, Z.; Cui, Y.; Liu, J.; Li, J.; Zhang, T. *Nat. Chem.* **2011**, *3*, 634.

(10) (a) Lin, J.; Qiao, B.; Liu, J.; Huang, Y.; Wang, A.; Li, L.; Zhang, W.; Allard, L.; Wang, X.; Zhang, T. *Angew. Chem., Int. Ed.* **2012**, *51*, 2920. (b) Uzun, A.; Ortalan, V.; Browning, N.; Gates, B. *Chem. Commun.* **2009**, 4657. (c) He, L.; Wang, J.; Gong, Y.; Liu, Y.; Cao, Y.; He, H.; Fan, K. *Angew. Chem., Int. Ed.* **2011**, *50*, 10216.

(11) Aydin, C.; Lu, J.; Browning, N.; Gates, B. *Angew. Chem., Int. Ed.* **2012**, *51*, 5929.

(12) Erdőhelyi, A.; Fodor, K.; Suru, G. *Appl. Catal., A* **1996**, *139*, 131.

(13) Sato, Y.; Soma, Y.; Miyao, T.; Naito, S. *Appl. Catal., A* **2006**, *304*, 78.

(14) Schweitzer, N.; Schaidle, J.; Ezekoye, O.; Pan, X.; Linic, S.; Thompson, L. *J. Am. Chem. Soc.* **2011**, *133*, 2378.

(15) Zhu, X.; Shen, M.; Lobban, L.; Mallinson, R. *J. Catal.* **2011**, *278*, 123.

(16) (a) Rodriguez, J.; Liu, P.; Hrbek, J.; Evans, J.; Pérez, M. *Angew. Chem., Int. Ed.* **2007**, *46*, 1329. (b) Shekhar, M.; Wang, J.; Lee, W.; Williams, W.; Kim, S.; Stach, E.; Miller, J.; Delgass, W.; Ribeiro, F.. *J. Am. Chem. Soc.* **2012**, *134*, 4700.

(17) (a) Liu, P.; Rodriguez, J. *J. Chem. Phys.* **2007**, *126*, 164705. (b) Averink Silberova, B.; Makkee, G.; Moulijn, J. *J. Catal.* **2006**, *243*, 171. (c) Gokhale, A.; Dumesic, J.; Mavrikakis, M. *J. Am. Chem. Soc.* **2008**, *130*, 1402.

(18) (a) Yang, M.; Allard, L.; Flytzani-Stephanopoulos, M. *J. Am. Chem. Soc.* **2013**, *135*, 3768. (b) Zhang, S.; Shan, J.; Zhu, Y.; Frenkel, A.; Patlolla, A.; Huang, W.; Yoon, S.; Wang, L.; Yoshida, H.; Takeda, S.; Tao, F. *J. Am. Chem. Soc.* **2013**, *135*, 8283.